

Search for a Neutral Higgs Boson Decaying to a W Boson Pair in $p\bar{p}$ Collisions at $\sqrt{s} = 1.96$ TeV

A. Abulencia,²³ D. Acosta,¹⁷ J. Adelman,¹³ T. Affolder,¹⁰ T. Akimoto,⁵⁵ M. G. Albrow,¹⁶ D. Ambrose,¹⁶ S. Amerio,⁴³ D. Amidei,³⁴ A. Anastassov,⁵² K. Anikeev,¹⁶ A. Annovi,¹⁸ J. Antos,¹ M. Aoki,⁵⁵ G. Apollinari,¹⁶ J.-F. Arguin,³³ T. Arisawa,⁵⁷ A. Artikov,¹⁴ W. Ashmanskas,¹⁶ A. Attal,⁸ F. Azfar,⁴² P. Azzi-Bacchetta,⁴³ P. Azzurri,⁴⁶ N. Bacchetta,⁴³ H. Bachacou,²⁸ W. Badgett,¹⁶ A. Barbaro-Galtieri,²⁸ V. E. Barnes,⁴⁸ B. A. Barnett,²⁴ S. Baroiant,⁷ V. Bartsch,³⁰ G. Bauer,³² F. Bedeschi,⁴⁶ S. Behari,²⁴ S. Belforte,⁵⁴ G. Bellettini,⁴⁶ J. Bellinger,⁵⁹ A. Belloni,³² E. Ben Haim,⁴⁴ D. Benjamin,¹⁵ A. Beretvas,¹⁶ J. Beringer,²⁸ T. Berry,²⁹ A. Bhatti,⁵⁰ M. Binkley,¹⁶ D. Bisello,⁴³ R. E. Blair,² C. Blocker,⁶ B. Blumenfeld,²⁴ A. Bocci,¹⁵ A. Bodek,⁴⁹ V. Boisvert,⁴⁹ G. Bolla,⁴⁸ A. Bolshov,³² D. Bortoletto,⁴⁸ J. Boudreau,⁴⁷ A. Boveia,¹⁰ B. Brau,¹⁰ C. Bromberg,³⁵ E. Brubaker,¹³ J. Budagov,¹⁴ H. S. Budd,⁴⁹ S. Budd,²³ K. Burkett,¹⁶ G. Busetto,⁴³ P. Bussey,²⁰ K. L. Byrum,² S. Cabrera,¹⁵ M. Campanelli,¹⁹ M. Campbell,³⁴ F. Canelli,⁸ A. Canepa,⁴⁸ D. Carlsmith,⁵⁹ R. Carosi,⁴⁶ S. Carron,¹⁵ M. Casarsa,⁵⁴ A. Castro,⁵ P. Catastini,⁴⁶ D. Cauz,⁵⁴ M. Cavalli-Sforza,³ A. Cerri,²⁸ L. Cerrito,⁴² S. H. Chang,²⁷ J. Chapman,³⁴ Y. C. Chen,¹ M. Chertok,⁷ G. Chiarelli,⁴⁶ G. Chlachidze,¹⁴ F. Chlebana,¹⁶ I. Cho,²⁷ K. Cho,²⁷ D. Chokheli,¹⁴ J. P. Chou,²¹ P. H. Chu,²³ S. H. Chuang,⁵⁹ K. Chung,¹² W. H. Chung,⁵⁹ Y. S. Chung,⁴⁹ M. Ciljak,⁴⁶ C. I. Ciobanu,²³ M. A. Ciocci,⁴⁶ A. Clark,¹⁹ D. Clark,⁶ M. Coca,¹⁵ G. Compostella,⁴³ M. E. Convery,⁵⁰ J. Conway,⁷ B. Cooper,³⁰ K. Copic,³⁴ M. Cordelli,¹⁸ G. Cortiana,⁴³ F. Cresciolo,⁴⁶ A. Cruz,¹⁷ C. Cuenca Almenar,⁷ J. Cuevas,¹¹ R. Culbertson,¹⁶ D. Cyr,⁵⁹ S. DaRonco,⁴³ S. D'Auria,²⁰ M. D'Onofrio,³ D. Dagenhart,⁶ P. de Barbaro,⁴⁹ S. De Cecco,⁵¹ A. Deisher,²⁸ G. De Lentdecker,⁴⁹ M. Dell'Orso,⁴⁶ F. Delli Paoli,⁴³ S. Demers,⁴⁹ L. Demortier,⁵⁰ J. Deng,¹⁵ M. Deninno,⁵ D. De Pedis,⁵¹ P. F. Derwent,¹⁶ C. Dionisi,⁵¹ J. R. Dittmann,⁴ P. DiTuro,⁵² C. Dörr,²⁵ S. Donati,⁴⁶ M. Donega,¹⁹ P. Dong,⁸ J. Donini,⁴³ T. Dorigo,⁴³ S. Dube,⁵² K. Ebina,⁵⁷ J. Efron,³⁹ J. Ehlers,¹⁹ R. Erbacher,⁷ D. Errede,²³ S. Errede,²³ R. Eusebi,¹⁶ H. C. Fang,²⁸ S. Farrington,²⁹ I. Fedorko,⁴⁶ W. T. Fedorko,¹³ R. G. Feild,⁶⁰ M. Feindt,²⁵ J. P. Fernandez,³¹ R. Field,¹⁷ G. Flanagan,⁴⁸ L. R. Flores-Castillo,⁴⁷ A. Foland,²¹ S. Forrester,⁷ G. W. Foster,¹⁶ M. Franklin,²¹ J. C. Freeman,²⁸ I. Furic,¹³ M. Gallinaro,⁵⁰ J. Galyardt,¹² J. E. Garcia,⁴⁶ M. Garcia Sciveres,²⁸ A. F. Garfinkel,⁴⁸ C. Gay,⁶⁰ H. Gerberich,²³ D. Gerdes,³⁴ S. Giagu,⁵¹ P. Giannetti,⁴⁶ A. Gibson,²⁸ K. Gibson,¹² C. Ginsburg,¹⁶ N. Giokaris,¹⁴ K. Giolo,⁴⁸ M. Giordani,⁵⁴ P. Giromini,¹⁸ M. Giunta,⁴⁶ G. Giurgiu,¹² V. Glagolev,¹⁴ D. Glenzinski,¹⁶ M. Gold,³⁷ N. Goldschmidt,³⁴ J. Goldstein,⁴² G. Gomez,¹¹ G. Gomez-Ceballos,¹¹ M. Goncharov,⁵³ O. González,³¹ I. Gorelov,³⁷ A. T. Goshaw,¹⁵ Y. Gotra,⁴⁷ K. Goulianos,⁵⁰ A. Gresele,⁴³ M. Griffiths,²⁹ S. Grinstein,²¹ C. Grosso-Pilcher,¹³ R. C. Group,¹⁷ U. Grundler,²³ J. Guimaraes da Costa,²¹ Z. Gunay-Unalan,³⁵ C. Haber,²⁸ S. R. Hahn,¹⁶ K. Hahn,⁴⁵ E. Halkiadakis,⁵² A. Hamilton,³³ B.-Y. Han,⁴⁹ J. Y. Han,⁴⁹ R. Handler,⁵⁹ F. Happacher,¹⁸ K. Hara,⁵⁵ M. Hare,⁵⁶ S. Harper,⁴² R. F. Harr,⁵⁸ R. M. Harris,¹⁶ K. Hatakeyama,⁵⁰ J. Hauser,⁸ C. Hays,¹⁵ A. Heijboer,⁴⁵ B. Heinemann,²⁹ J. Heinrich,⁴⁵ M. Herndon,⁵⁹ D. Hidas,¹⁵ C. S. Hill,¹⁰ D. Hirschbuehl,²⁵ A. Hocker,¹⁶ A. Holloway,²¹ S. Hou,¹ M. Houlden,²⁹ S.-C. Hsu,⁹ B. T. Huffman,⁴² R. E. Hughes,³⁹ J. Huston,³⁵ J. Incandela,¹⁰ G. Introzzi,⁴⁶ M. Iori,⁵¹ Y. Ishizawa,⁵⁵ A. Ivanov,⁷ B. Iyutin,³² E. James,¹⁶ D. Jang,⁵² B. Jayatilaka,³⁴ D. Jeans,⁵¹ H. Jensen,¹⁶ E. J. Jeon,²⁷ S. Jindariani,¹⁷ M. Jones,⁴⁸ K. K. Joo,²⁷ S. Y. Jun,¹² T. R. Junk,²³ T. Kamon,⁵³ J. Kang,³⁴ P. E. Karchin,⁵⁸ Y. Kato,⁴¹ Y. Kemp,²⁵ R. Kephart,¹⁶ U. Kerzel,²⁵ V. Khotilovich,⁵³ B. Kilminster,³⁹ D. H. Kim,²⁷ H. S. Kim,²⁷ J. E. Kim,²⁷ M. J. Kim,¹² S. B. Kim,²⁷ S. H. Kim,⁵⁵ Y. K. Kim,¹³ L. Kirsch,⁶ S. Klimenko,¹⁷ M. Klute,³² B. Knuteson,³² B. R. Ko,¹⁵ H. Kobayashi,⁵⁵ K. Kondo,⁵⁷ D. J. Kong,²⁷ J. Konigsberg,¹⁷ A. Korytov,¹⁷ A. V. Kotwal,¹⁵ A. Kovalev,⁴⁵ A. Kraan,⁴⁵ J. Kraus,²³ I. Kravchenko,³² M. Kreps,²⁵ J. Kroll,⁴⁵ N. Krumnack,⁴ M. Kruse,¹⁵ V. Krutelyov,⁵³ S. E. Kuhlmann,² Y. Kusakabe,⁵⁷ S. Kwang,¹³ A. T. Laasanen,⁴⁸ S. Lai,³³ S. Lami,⁴⁶ S. Lammel,¹⁶ M. Lancaster,³⁰ R. L. Lander,⁷ K. Lannon,³⁹ A. Lath,⁵² G. Latino,⁴⁶ I. Lazzizzera,⁴³ T. LeCompte,² J. Lee,⁴⁹ J. Lee,²⁷ Y. J. Lee,²⁷ S. W. Lee,⁵³ R. Lefèvre,³ N. Leonardo,³² S. Leone,⁴⁶ S. Levy,¹³ J. D. Lewis,¹⁶ C. Lin,⁶⁰ C. S. Lin,¹⁶ M. Lindgren,¹⁶ E. Lipeles,⁹ T. M. Liss,²³ A. Lister,¹⁹ D. O. Litvintsev,¹⁶ T. Liu,¹⁶ N. S. Lockyer,⁴⁵ A. Loginov,³⁶ M. Loreti,⁴³ P. Loverre,⁵¹ R.-S. Lu,¹ D. Lucchesi,⁴³ P. Lujan,²⁸ P. Lukens,¹⁶ G. Lungu,¹⁷ L. Lyons,⁴² J. Lys,²⁸ R. Lysak,¹ E. Lytken,⁴⁸ P. Mack,²⁵ D. MacQueen,³³ R. Madrak,¹⁶ K. Maeshima,¹⁶ T. Maki,²² P. Maksimovic,²⁴ S. Malde,⁴² G. Manca,²⁹ F. Margaroli,⁵ R. Marginean,¹⁶ C. Marino,²³ A. Martin,⁶⁰ V. Martin,³⁸ M. Martínez,³ T. Maruyama,⁵⁵ P. Mastrandrea,⁵¹ H. Matsunaga,⁵⁵ M. E. Mattson,⁵⁸ R. Mazini,³³ P. Mazzanti,⁵ K. S. McFarland,⁴⁹ P. McIntyre,⁵³ R. McNulty,²⁹ A. Mehta,²⁹ S. Menzemer,¹¹ A. Menzione,⁴⁶ P. Merkel,⁴⁸ C. Mesropian,⁵⁰ A. Messina,⁵¹ M. von der Mey,⁸ T. Miao,¹⁶ N. Miladinovic,⁶ J. Miles,³² R. Miller,³⁵ J. S. Miller,³⁴ C. Mills,¹⁰ M. Milnik,²⁵ R. Miquel,²⁸ A. Mitra,¹ G. Mitselmakher,¹⁷ A. Miyamoto,²⁶ N. Moggi,⁵ B. Mohr,⁸ R. Moore,¹⁶ M. Morello,⁴⁶ P. Movilla Fernandez,²⁸ J. Mülmenstädt,²⁸ A. Mukherjee,¹⁶ Th. Muller,²⁵ R. Mumford,²⁴ P. Murat,¹⁶ J. Nachtman,¹⁶ J. Naganoma,⁵⁷ S. Nahn,³² I. Nakano,⁴⁰ A. Napier,⁵⁶ D. Naumov,³⁷ V. Necula,¹⁷ C. Neu,⁴⁵ M. S. Neubauer,⁹ J. Nielsen,²⁸ T. Nigmanov,⁴⁷

L. Nodulman,² O. Norriella,³ E. Nurse,³⁰ T. Ogawa,⁵⁷ S. H. Oh,¹⁵ Y. D. Oh,²⁷ T. Okusawa,⁴¹ R. Oldeman,²⁹ R. Orava,²² K. Osterberg,²² C. Pagliarone,⁴⁶ E. Palencia,¹¹ R. Paoletti,⁴⁶ V. Papadimitriou,¹⁶ A. A. Paramonov,¹³ B. Parks,³⁹ S. Pashapour,³³ J. Patrick,¹⁶ G. Pauletta,⁵⁴ M. Paulini,¹² C. Paus,³² D. E. Pellett,⁷ A. Penzo,⁵⁴ T. J. Phillips,¹⁵ G. Piacentino,⁴⁶ J. Piedra,⁴⁴ L. Pinera,¹⁷ K. Pitts,²³ C. Plager,⁸ L. Pondrom,⁵⁹ X. Portell,³ O. Poukhov,¹⁴ N. Pounder,⁴² F. Prakošhyn,¹⁴ A. Pronko,¹⁶ J. Proudfoot,² F. Ptohos,¹⁸ G. Punzi,⁴⁶ J. Pursley,²⁴ J. Rademacker,⁴² A. Rahaman,⁴⁷ A. Rakitin,³² S. Rappoccio,²¹ F. Ratnikov,⁵² B. Reiser,¹⁶ V. Rekovic,³⁷ N. van Remortel,²² P. Renton,⁴² M. Rescigno,⁵¹ S. Richter,²⁵ F. Rimondi,⁵ L. Ristori,⁴⁶ W. J. Robertson,¹⁵ A. Robson,²⁰ T. Rodrigo,¹¹ E. Rogers,²³ S. Rolli,⁵⁶ R. Roser,¹⁶ M. Rossi,⁵⁴ R. Rossin,¹⁷ C. Rott,⁴⁸ A. Ruiz,¹¹ J. Russ,¹² V. Rusu,¹³ H. Saarikko,²² S. Sabik,³³ A. Safonov,⁵³ W. K. Sakumoto,⁴⁹ G. Salamanna,⁵¹ O. Saltó,³ D. Saltzberg,⁸ C. Sanchez,³ L. Santi,⁵⁴ S. Sarkar,⁵¹ L. Sartori,⁴⁶ K. Sato,⁵⁵ P. Savard,³³ A. Savoy-Navarro,⁴⁴ T. Scheidle,²⁵ P. Schlabach,¹⁶ E. E. Schmidt,¹⁶ M. P. Schmidt,⁶⁰ M. Schmitt,³⁸ T. Schwarz,³⁴ L. Scodellaro,¹¹ A. L. Scott,¹⁰ A. Scribano,⁴⁶ F. Scuri,⁴⁶ A. Sedov,⁴⁸ S. Seidel,³⁷ Y. Seiya,⁴¹ A. Semenov,¹⁴ L. Sexton-Kennedy,¹⁶ I. Sfiligoi,¹⁸ M. D. Shapiro,²⁸ T. Shears,²⁹ P. F. Shepard,⁴⁷ D. Sherman,²¹ M. Shimojima,⁵⁵ M. Shochet,¹³ Y. Shon,⁵⁹ I. Shreyber,³⁶ A. Sidoti,⁴⁴ P. Sinervo,³³ A. Sisakyan,¹⁴ J. Sjolín,⁴² A. Skiba,²⁵ A. J. Slaughter,¹⁶ K. Sliwa,⁵⁶ J. R. Smith,⁷ F. D. Snider,¹⁶ R. Snihur,³³ M. Soderberg,³⁴ A. Soha,⁷ S. Somalwar,⁵² V. Sorin,³⁵ J. Spalding,¹⁶ M. Spezziga,¹⁶ F. Spinella,⁴⁶ T. Spreitzer,³³ P. Squillacioti,⁴⁶ M. Stanitzki,⁶⁰ A. Staveris-Polykalas,⁴⁶ R. St. Denis,²⁰ B. Stelzer,⁸ O. Stelzer-Chilton,⁴² D. Stentz,³⁸ J. Strologas,³⁷ D. Stuart,¹⁰ J. S. Suh,²⁷ A. Sukhanov,¹⁷ K. Sumorok,³² H. Sun,⁵⁶ T. Suzuki,⁵⁵ A. Taffard,²³ R. Takashima,⁴⁰ Y. Takeuchi,⁵⁵ K. Takikawa,⁵⁵ M. Tanaka,² R. Tanaka,⁴⁰ N. Tanimoto,⁴⁰ M. Tecchio,³⁴ P. K. Teng,¹ K. Terashi,⁵⁰ S. Tether,³² J. Thom,¹⁶ A. S. Thompson,²⁰ E. Thomson,⁴⁵ P. Tipton,⁴⁹ V. Tiwari,¹² S. Tkaczyk,¹⁶ D. Toback,⁵³ S. Tokar,¹⁴ K. Tollefson,³⁵ T. Tomura,⁵⁵ D. Tonelli,⁴⁶ M. Tönnesmann,³⁵ S. Torre,¹⁸ D. Torretta,¹⁶ S. Tourneur,⁴⁴ W. Trischuk,³³ R. Tsuchiya,⁵⁷ S. Tsuno,⁴⁰ N. Turini,⁴⁶ F. Ukegawa,⁵⁵ T. Unverhau,²⁰ S. Uozumi,⁵⁵ D. Usynin,⁴⁵ A. Vaiciulis,⁴⁹ S. Vallecorsa,¹⁹ A. Varganov,³⁴ E. Vataga,³⁷ G. Velev,¹⁶ G. Veramendi,²³ V. Veszpremi,⁴⁸ R. Vidal,¹⁶ I. Vila,¹¹ R. Vilar,¹¹ T. Vine,³⁰ I. Vollrath,³³ I. Volobouev,²⁸ G. Volpi,⁴⁶ F. Würthwein,⁹ P. Wagner,⁵³ R. G. Wagner,² R. L. Wagner,¹⁶ W. Wagner,²⁵ R. Wallny,⁸ T. Walter,²⁵ Z. Wan,⁵² S. M. Wang,¹ A. Warburton,³³ S. Waschke,²⁰ D. Waters,³⁰ W. C. Wester III,¹⁶ B. Whitehouse,⁵⁶ D. Whiteson,⁴⁵ A. B. Wicklund,² E. Wicklund,¹⁶ G. Williams,³³ H. H. Williams,⁴⁵ P. Wilson,¹⁶ B. L. Winer,³⁹ P. Wittich,¹⁶ S. Wolbers,¹⁶ C. Wolfe,¹³ T. Wright,³⁴ X. Wu,¹⁹ S. M. Wynne,²⁹ A. Yagil,¹⁶ K. Yamamoto,⁴¹ J. Yamaoka,⁵² T. Yamashita,⁴⁰ C. Yang,⁶⁰ U. K. Yang,¹³ Y. C. Yang,²⁷ W. M. Yao,²⁸ G. P. Yeh,¹⁶ J. Yoh,¹⁶ K. Yorita,¹³ T. Yoshida,⁴¹ G. B. Yu,⁴⁹ I. Yu,²⁷ S. S. Yu,¹⁶ J. C. Yun,¹⁶ L. Zanello,⁵¹ A. Zanelti,⁵⁴ I. Zaw,²¹ F. Zetti,⁴⁶ X. Zhang,²³ J. Zhou,⁵² and S. Zucchelli⁵

(CDF Collaboration)

¹*Institute of Physics, Academia Sinica, Taipei, Taiwan 11529, Republic of China*²*Argonne National Laboratory, Argonne, Illinois 60439, USA*³*Institut de Física d'Altes Energies, Universitat Autònoma de Barcelona, E-08193 Bellaterra (Barcelona), Spain*⁴*Baylor University, Waco, Texas 76798, USA*⁵*Istituto Nazionale di Fisica Nucleare, University of Bologna, I-40127 Bologna, Italy*⁶*Brandeis University, Waltham, Massachusetts 02254, USA*⁷*University of California, Davis, Davis, California 95616, USA*⁸*University of California, Los Angeles, Los Angeles, California 90024, USA*⁹*University of California, San Diego, La Jolla, California 92093, USA*¹⁰*University of California, Santa Barbara, Santa Barbara, California 93106, USA*¹¹*Instituto de Física de Cantabria, CSIC-University of Cantabria, 39005 Santander, Spain*¹²*Carnegie Mellon University, Pittsburgh, Pennsylvania 15213, USA*¹³*Enrico Fermi Institute, University of Chicago, Chicago, Illinois 60637, USA*¹⁴*Joint Institute for Nuclear Research, RU-141980 Dubna, Russia*¹⁵*Duke University, Durham, North Carolina 27708, USA*¹⁶*Fermi National Accelerator Laboratory, Batavia, Illinois 60510, USA*¹⁷*University of Florida, Gainesville, Florida 32611, USA*¹⁸*Laboratori Nazionali di Frascati, Istituto Nazionale di Fisica Nucleare, I-00044 Frascati, Italy*¹⁹*University of Geneva, CH-1211 Geneva 4, Switzerland*²⁰*Glasgow University, Glasgow G12 8QQ, United Kingdom*²¹*Harvard University, Cambridge, Massachusetts 02138, USA*²²*Division of High Energy Physics, Department of Physics, University of Helsinki and Helsinki Institute of Physics, FIN-00014 Helsinki, Finland*²³*University of Illinois, Urbana, Illinois 61801, USA*

- ²⁴The Johns Hopkins University, Baltimore, Maryland 21218, USA
- ²⁵Institut für Experimentelle Kernphysik, Universität Karlsruhe, 76128 Karlsruhe, Germany
- ²⁶High Energy Accelerator Research Organization (KEK), Tsukuba, Ibaraki 305, Japan
- ²⁷Center for High Energy Physics: Kyungpook National University, Taegu 702-701, Korea;
Seoul National University, Seoul 151-742, Korea;
and SungKyunKwan University, Suwon 440-746, Korea
- ²⁸Ernest Orlando Lawrence Berkeley National Laboratory, Berkeley, California 94720, USA
- ²⁹University of Liverpool, Liverpool L69 7ZE, United Kingdom
- ³⁰University College London, London WC1E 6BT, United Kingdom
- ³¹Centro de Investigaciones Energeticas Medioambientales y Tecnológicas, E-28040 Madrid, Spain
- ³²Massachusetts Institute of Technology, Cambridge, Massachusetts 02139, USA
- ³³Institute of Particle Physics: McGill University, Montréal, Canada H3A 2T8;
and University of Toronto, Toronto, Canada M5S 1A7
- ³⁴University of Michigan, Ann Arbor, Michigan 48109, USA
- ³⁵Michigan State University, East Lansing, Michigan 48824, USA
- ³⁶Institution for Theoretical and Experimental Physics, ITEP, Moscow 117259, Russia
- ³⁷University of New Mexico, Albuquerque, New Mexico 87131, USA
- ³⁸Northwestern University, Evanston, Illinois 60208, USA
- ³⁹The Ohio State University, Columbus, Ohio 43210, USA
- ⁴⁰Okayama University, Okayama 700-8530, Japan
- ⁴¹Osaka City University, Osaka 588, Japan
- ⁴²University of Oxford, Oxford OX1 3RH, United Kingdom
- ⁴³Istituto Nazionale di Fisica Nucleare, University of Padova, Sezione di Padova-Trento, I-35131 Padova, Italy
- ⁴⁴LPNHE, Université Pierre et Marie Curie/IN2P3-CNRS, UMR7585, Paris F-75252, France
- ⁴⁵University of Pennsylvania, Philadelphia, Pennsylvania 19104, USA
- ⁴⁶Istituto Nazionale di Fisica Nucleare Pisa, Universities of Pisa, Siena and Scuola Normale Superiore, I-56127 Pisa, Italy
- ⁴⁷University of Pittsburgh, Pittsburgh, Pennsylvania 15260, USA
- ⁴⁸Purdue University, West Lafayette, Indiana 47907, USA
- ⁴⁹University of Rochester, Rochester, New York 14627, USA
- ⁵⁰The Rockefeller University, New York, New York 10021, USA
- ⁵¹Istituto Nazionale di Fisica Nucleare, Sezione di Roma 1, University of Rome “La Sapienza,” I-00185 Roma, Italy
- ⁵²Rutgers University, Piscataway, New Jersey 08855, USA
- ⁵³Texas A&M University, College Station, Texas 77843, USA
- ⁵⁴Istituto Nazionale di Fisica Nucleare, University of Trieste/Udine, Italy
- ⁵⁵University of Tsukuba, Tsukuba, Ibaraki 305, Japan
- ⁵⁶Tufts University, Medford, Massachusetts 02155, USA
- ⁵⁷Waseda University, Tokyo 169, Japan
- ⁵⁸Wayne State University, Detroit, Michigan 48201, USA
- ⁵⁹University of Wisconsin, Madison, Wisconsin 53706, USA
- ⁶⁰Yale University, New Haven, Connecticut 06520, USA

(Received 31 May 2006; published 25 August 2006)

We present the results of a search for standard model Higgs boson production with decay to WW^* , identified through the leptonic final states $e^+e^-\bar{\nu}\nu$, $e^\pm\mu^\mp\bar{\nu}\nu$ and $\mu^+\mu^-\bar{\nu}\nu$. This search uses 360 pb^{-1} of data collected from $p\bar{p}$ collisions at $\sqrt{s} = 1.96\text{ TeV}$ by the upgraded Collider Detector at Fermilab (CDF II). We observe no signal excess and set 95% confidence level upper limits on the production cross section times branching ratio for the Higgs boson to WW^* or any new scalar particle with similar decay products. These upper limits range from 5.5 to 3.2 pb for Higgs boson masses between 120 and 200 GeV/ c^2 .

DOI: [10.1103/PhysRevLett.97.081802](https://doi.org/10.1103/PhysRevLett.97.081802)

PACS numbers: 14.80.Bn, 13.85.Ni, 13.85.Qk, 13.85.Rm

The Higgs mechanism is a leading candidate for electroweak symmetry breaking and consequently for mass generation of the W and Z bosons without violation of local gauge invariance. A manifestation of this mechanism is the existence of a neutral scalar particle, the Higgs boson [1], which has not been observed to date. Its mass is a free parameter in the standard model (SM),

but its couplings to other particles of known mass are fully specified at tree level. Direct searches at the CERN e^+e^- collider (LEP) yielded a lower limit for the Higgs boson mass of $m_H > 114.4\text{ GeV}/c^2$ at 95% confidence level (C.L.) [2]. Precision electroweak measurements indirectly predict a Higgs boson mass of $91^{+45}_{-32}\text{ GeV}/c^2$ [3].

At the Tevatron, the dominant production mechanism for the SM Higgs boson is gluon-gluon fusion through heavy quark loops. Branching fractions for the various decay channels of the Higgs boson depend on its mass. For masses below about $135 \text{ GeV}/c^2$ the dominant decay is $H \rightarrow b\bar{b}$, while heavier Higgs bosons decay predominantly to WW^* [4], where W^* indicates a W boson that can be off mass shell. For the $b\bar{b}$ decay mode, the requirement of associated production of the Higgs boson with vector bosons ($p\bar{p} \rightarrow WH/ZH$) can greatly improve the signal purity [5]. For the WW^* decay mode, the leptonic decays of W bosons give a clean enough signature that the inclusive single Higgs production process gives the best search sensitivity. The next-to-leading order (NLO) production cross section [4] times branching ratio for a SM Higgs boson, $\sigma(p\bar{p} \rightarrow H) \times \text{BR}(H \rightarrow WW^*)$, ranges from 0.036 to 0.25 pb for Higgs masses of 110–200 GeV/c^2 .

This Letter presents the results of a direct search for a Higgs boson in the channel $gg \rightarrow H \rightarrow WW^* \rightarrow \ell^+ \nu \ell^- \bar{\nu}$ ($\ell = e, \mu, \tau$), identified by the “dilepton” final states e^+e^- , $e^\pm\mu^\mp$, or $\mu^+\mu^-$. We also include the efficiency for leptonically decaying taus to e or μ . This is the first search in this channel by the CDF Collaboration. A similar search in this channel was recently performed by the D0 Collaboration [6]. The data sample used for this analysis were collected with the CDF II detector at the Fermilab Tevatron between 2002 and 2004, and corresponds to an integrated luminosity of approximately 360 pb^{-1} [7]. For this integrated luminosity, the cross-section limits we are able to place on Higgs production are a factor of approximately 10–50 larger than the SM expectation, based on the NLO calculation. However, the production cross section can be enhanced in extensions to the SM due to new particles, e.g., a fourth generation fermion family [8], contributing at higher order to the gluon-gluon fusion Higgs production process.

CDF II is a detector with approximate azimuthal and forward-backward symmetry and it is fully described elsewhere [9]. It consists of a charged-particle tracking system in a 1.4 T magnetic field and segmented electromagnetic and hadronic calorimeters surrounded by muon detectors. The electromagnetic and hadronic sampling calorimeters surrounding the solenoid are used to measure the energy of interacting particles in the pseudorapidity range $|\eta| < 3.6$ [10]. The calorimeters are divided into projective geometry towers. This analysis uses both central ($|\eta| < 1.1$) and end-plug detectors ($1.2 < |\eta| < 2.0$) to identify electron candidates. A set of drift chambers located outside the central hadron calorimeters and another set behind a 60 cm iron shield help detect muons in the region $|\eta| < 0.6$. Additional drift chambers and scintillation counters detect muons in the region $0.6 \leq |\eta| \leq 1.0$.

Events used for this analysis are collected using the following triggers [11,12]: an inclusive central electron ($|\eta| < 1.1$) trigger requiring an electron with $E_T >$

18 GeV, an inclusive central muon ($|\eta| < 1.0$) trigger requiring a muon with $p_T > 18 \text{ GeV}/c$, or a trigger for events with a forward electron ($1.2 \leq |\eta| \leq 2.0$) with $E_T > 20 \text{ GeV}$ and missing transverse energy, $\cancel{E}_T > 15 \text{ GeV}$ [13].

After the event reconstruction, event selection criteria which retain high $H \rightarrow WW^*$ signal efficiency while minimizing the effect of background contamination are applied. Some selection requirements are mass dependent, as the event kinematics and topology change as functions of m_H .

The selection requires two oppositely charged lepton candidates originating from the same vertex, with $p_T > 20 \text{ GeV}/c$ for the trigger lepton and $p_T > 10 \text{ GeV}/c$ for the second one. The leptons are also required to be isolated in both the calorimeter and the tracking chamber [14], and the dilepton invariant mass $m_{\ell\ell}$ is required to be greater than $16 \text{ GeV}/c^2$, in order to remove events from the $c\bar{c}/b\bar{b}$ resonances.

After removal of events identified as cosmic rays or electrons from photon conversions [11], we count the jets [15] with $E_T > 15 \text{ GeV}$ and $|\eta| < 2.5$. Signal events do not typically have high- E_T jets in the final state, but can occasionally have lower- E_T jets from initial state gluon radiation. On the other hand, $t\bar{t}$ pairs decay primarily to $W^+W^-b\bar{b}$ and thus tend to have at least two jets in the final state. This background is reduced by selecting only events satisfying one of the following criteria: no jets with $E_T > 15 \text{ GeV}$, or only one jet with $15 < E_T < 55 \text{ GeV}$, or two jets each with $15 < E_T < 40 \text{ GeV}$. Events with more than two jets with $E_T > 15 \text{ GeV}$ are also rejected.

After the selection criteria described above, the dominant surviving background is Drell-Yan production of $\ell^+\ell^-$ pairs, which is suppressed by requiring that $\cancel{E}_T > m_H/4$. The events with missing energy due to a mismeasurement of the jet energy, or $Z \rightarrow \tau\tau$ events with missing energy arising from a leptonic tau decay, are removed by requiring the azimuthal angle between the \cancel{E}_T and the closest jet or lepton to be at least 20° , if $\cancel{E}_T < 50 \text{ GeV}$. To further reduce the large Z/γ^* background, the dilepton invariant mass is required to be $m_{\ell\ell} < (m_H/2 - 5) \text{ GeV}/c^2$. Finally, the scalar sum of the p_T of the two leptons and the \cancel{E}_T is required to be below the Higgs boson mass.

The kinematic cuts described above exploit the correlations in the W pairs produced by the decay of a Higgs boson and suppress SM WW production. These correlations are due to angular momentum conservation in the decay of a spin-zero Higgs boson. Since W bosons decay into left-handed leptons and right-handed antileptons, and since the W bosons in the decay $H \rightarrow WW^*$ have opposite helicities, the final state lepton pairs and also the neutrino pairs tend to be azimuthally aligned in Higgs decay. This implies that the signal events tend to have smaller $m_{\ell\ell}$ and azimuthal angle between leptons ($\Delta\phi$) and larger \cancel{E}_T , as compared with production of SM WW pairs. These differ-

TABLE I. The branching ratio $BR(H \rightarrow WW^*)$ and the total acceptance of the signal after all the selection criteria. The total acceptance is calculated with respect to the number of $p\bar{p} \rightarrow H \rightarrow WW^* \rightarrow \ell^+ \nu \ell^- \bar{\nu}$ events.

m_H (GeV/ c^2)	120	140	160	180	200
$BR(H \rightarrow WW^*)$ (%)	13	48	90	94	74
Total acceptance (%)	3.15	4.56	6.47	6.41	5.54

ences are further exploited in the final stages of the analysis, when the $\Delta\phi$ distribution of the data is compared with the background and signal predictions.

The acceptance for identifying $H \rightarrow WW^* \rightarrow \ell\nu\ell\nu$ events with the above selection criteria is calculated as a function of the Higgs boson mass using the PYTHIA [16] Monte Carlo program, after a GEANT-based [17] simulation of the CDF detector response. The total acceptance is a product of the geometric and kinematic acceptance, the lepton identification efficiencies, the trigger efficiencies, and the topological cut efficiencies. It does not include the branching fraction of W leptonic decays. The total acceptance ranges from 3.0% to 6.5%, depending on the Higgs mass, and is summarized in Table I. Approximately 25% of the expected signal are ee events, 25% $\mu\mu$, and 50% $e\mu$.

The systematic uncertainty on the acceptance is 6% resulting from uncertainties in the modeling of the initial state radiation by PYTHIA (3%), and uncertainties on the gluon parton distribution functions (4%) [18], jet energy scale (1%), track isolation (<2%), electron and muon trigger efficiencies (<1%), and electron and muon identification efficiencies (2%). In addition, a 6% uncertainty on the integrated luminosity is applied to the expected number of events for all processes [19].

After all selection requirements, the background events come predominantly from WW pair production (about 70% of the total for $m_H = 160$ GeV/ c^2) [20], Z/γ^* , $W + \text{jets}$, and $W + \gamma$. Smaller backgrounds include WZ , ZZ , and $t\bar{t}$ production. A summary of these contributions as a function of Higgs mass is given in Table II. The diboson (WW , WZ , ZZ), Z/γ^* , and $t\bar{t}$ backgrounds are determined using the PYTHIA Monte Carlo program, followed by the

TABLE II. The expected number of signal and SM background events are presented. The number of events observed in the data, with the m_H dependent selection criteria, is also shown. The errors include all systematic effects.

m_H (GeV/ c^2)	120	140	160	180	200
WW	5.49 ± 0.66	7.98 ± 0.96	9.79 ± 1.18	9.89 ± 1.19	9.19 ± 1.11
Z/γ^*	1.63 ± 0.42	1.01 ± 0.26	0.76 ± 0.20	0.83 ± 0.21	0.96 ± 0.25
$W + \text{jets}/\gamma$	4.57 ± 0.90	3.49 ± 0.81	2.48 ± 0.69	1.70 ± 0.46	1.20 ± 0.37
$WZ + ZZ$	0.25 ± 0.03	0.37 ± 0.05	0.40 ± 0.05	0.49 ± 0.07	1.16 ± 0.15
$t\bar{t}$	0.12 ± 0.01	0.21 ± 0.02	0.35 ± 0.04	0.46 ± 0.05	0.58 ± 0.06
Total background	12.06 ± 1.19	13.08 ± 1.28	13.78 ± 1.38	13.37 ± 1.30	13.09 ± 1.21
$H \rightarrow WW^*$	0.090 ± 0.008	0.32 ± 0.03	0.58 ± 0.05	0.41 ± 0.03	0.20 ± 0.02
Data	7	14	16	19	17

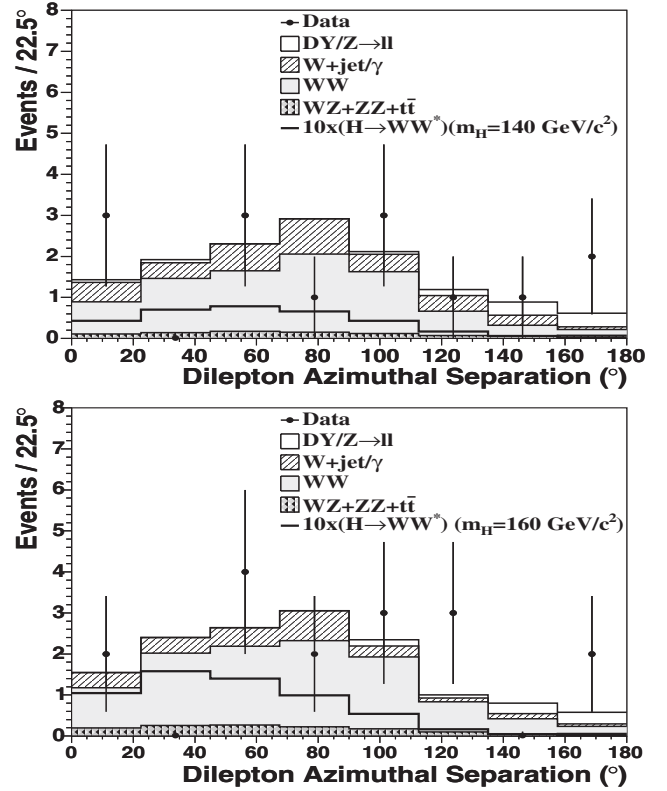


FIG. 1. Dilepton azimuthal distributions for SM backgrounds, HWW signal, and data, for two Higgs masses: 140 GeV/ c^2 (top panel) and 160 GeV/ c^2 (bottom panel). Note that the Higgs signal is scaled by a factor of 10 and is not included in the cumulative background distributions.

CDF II detector simulation. We normalize the total number of events for these processes to recent theoretical cross sections [21,22]. To estimate the $W + \gamma$ background we use a matrix element generator [23] and use PYTHIA for the initial state QCD radiation and hadronization.

The background from $W + \text{jets}$, where a jet or track is misidentified as a lepton (electron or muon), is determined from the data and called the “fake background.” We first determine the probability that a jet with a large fraction of its energy deposited in the electromagnetic calorimeter is

TABLE III. The expected and observed 95% C.L. limits on $\sigma(p\bar{p} \rightarrow H) \times \text{BR}(H \rightarrow WW^*)$.

m_H (GeV/ c^2)	120	140	160	180	200
Expected limits (pb)	7.1	4.8	3.5	3.4	4.0
Observed limits (pb)	4.5	4.6	3.2	4.3	5.2

misidentified as an electron, and the probability that a minimum ionizing track is misidentified as a muon. These probabilities are termed fake rates. The fake rate for each lepton type is calculated using an average of four inclusive jet samples (triggered with at least one jet with $E_T > 20, 50, 70,$ or 100 GeV). We subtract the contribution from sources of real leptons (W and Z decays) and parametrize the fake rates as a function of jet transverse energy (for electrons) or track transverse momentum (for muons). The background is determined by weighting the jets from a data sample of ($W \rightarrow \ell\nu$) + jets events by the fake rates.

For data events passing the previously described selection criteria, we search for an excess of events in the azimuthal angle distribution between the leptons, $\Delta\phi$. A binned likelihood is used to compare the azimuthal angle distribution in the data with a combination of expected distributions from the SM background processes. Figure 1 shows the $\Delta\phi$ distributions for SM backgrounds, for Higgs masses of 140 and 160 GeV/ c^2 , and for the data. We observe no evidence for a signal over the SM expectations. We calculate upper limits on the production cross section times branching ratio, $\sigma_H \times \text{BR}(H \rightarrow WW^*)$, using a Bayesian procedure. We consider three components in the data: $H \rightarrow WW^*$, SM WW , and other SM processes ($WZ, ZZ, \text{Drell-Yan}, W + \text{jets}/\gamma$) labeled as ‘‘other.’’ The expected number of events in each $\Delta\phi$ bin is

$$\mu = f_{WW}n_{WW} + f_{\text{other}}n_{\text{other}} + f_{HWW}[\epsilon\mathcal{L}\sigma_H\text{BR}(H \rightarrow WW^*)],$$

where f_{WW} , f_{other} , and f_{HWW} represent the expected fraction of the specified categories of events falling in each $\Delta\phi$ bin, n_{WW} and n_{other} are the expected numbers of WW and non- WW background events, and ϵ , \mathcal{L} , and σ_H correspond to efficiency, integrated luminosity, and H production cross section. A posterior density is obtained by multiplying the Poisson likelihood function with Gaussian prior densities for the integrated luminosity, background normalizations, and the signal efficiency:

$$L = \prod_{i=1}^{N_{\text{bins}}} \frac{\mu_i^{n_i} e^{-\mu_i}}{n_i!} G(n_{WW}, \sigma_{WW}) G(n_{\text{other}}, \sigma_{\text{other}}) \times G(\epsilon, \sigma_\epsilon) G(\mathcal{L}, \sigma_{\mathcal{L}}),$$

where n_i is the number of events observed in the data, and $G(n, \sigma_n)$ are Gaussian constraints for parameter n with

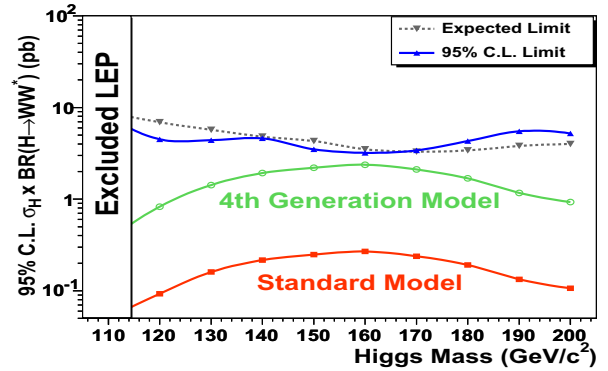


FIG. 2 (color online). Summary of the run II CDF 95% C.L. upper limits on $\sigma(p\bar{p} \rightarrow H) \times \text{BR}(H \rightarrow WW^*)$. Shown for comparison are the standard model prediction, the fourth generation model prediction [8], and the region excluded by the LEP experiments. The prediction for the fourth generation model assumes that fourth family fermions have a mass $m_4 = 200$ GeV/ c^2 .

uncertainty σ_n . The prior density for $\sigma \times \text{BR}(H \rightarrow WW^*)$ is assumed uniform. The posterior density is then integrated over all parameters except for $\sigma \times \text{BR}(H \rightarrow WW^*)$, for which a 95% C.L. upper limit is obtained by calculating the 95th percentile of the resulting distribution.

The expected and observed upper limits on the cross section times branching ratio, $\sigma \times \text{BR}(H \rightarrow WW^*)$, for different Higgs masses are shown in Table III. The expected limits are calculated using 1000 simulated experiments, assuming no signal, for each Higgs mass. The median value of the limits obtained from these experiments is chosen as the *a priori* upper limit.

In conclusion, observing no signal in the direct search for $H \rightarrow WW^*$, with the subsequent decay of the W bosons to leptons, we have set mass dependent limits at 95% C.L. on $\sigma(p\bar{p} \rightarrow H) \times \text{BR}(H \rightarrow WW^*)$. This search is potentially sensitive to other new physics models such as the example in Fig. 2.

We thank the Fermilab staff and the technical staffs of the participating institutions for their vital contributions. This work was supported by the U.S. Department of Energy and National Science Foundation; the Italian Istituto Nazionale di Fisica Nucleare; the Ministry of Education, Culture, Sports, Science and Technology of Japan; the Natural Sciences and Engineering Research Council of Canada; the National Science Council of the Republic of China; the Swiss National Science Foundation; the A. P. Sloan Foundation; the Bundesministerium für Bildung und Forschung, Germany; the Korean Science and Engineering Foundation and the Korean Research Foundation; the Particle Physics and Astronomy Research Council and the Royal Society, U.K.; the Russian Foundation for Basic Research; the Comisión Interministerial de Ciencia y Tecnología, Spain; in part by the European Community’s Human Potential

Programme under Contract No. HPRN-CT-2002-00292; and the Academy of Finland.

-
- [1] P. W. Higgs, *Phys. Lett.* **12**, 132 (1964).
- [2] R. Barate *et al.* (ALEPH Collaboration), *Phys. Lett. B* **565**, 61 (2003).
- [3] J. Alcaraz *et al.*, hep-ex/0511027.
- [4] A. Djouadi, J. Kalinowski, and M. Spira, *Comput. Phys. Commun.* **108**, 56 (1998); S. Catani, D. de Florian, M. Grazzini, and P. Nason, *J. High Energy Phys.* **07** (2003) 028.
- [5] D. Acosta *et al.* (CDF Collaboration), *Phys. Rev. Lett.* **95**, 051801 (2005); A. Abulencia *et al.* (CDF Collaboration), *Phys. Rev. Lett.* **96**, 081803 (2006).
- [6] V. M. Abazov *et al.* (D0 Collaboration), *Phys. Rev. Lett.* **96**, 011801 (2006).
- [7] The integrated luminosities for ee , $e\mu$, and $\mu\mu$ are 363 ± 22 , 356 ± 21 , and 364 ± 22 pb^{-1} , respectively. The differences for the various channels are due to different detector quality requirements.
- [8] E. Arik *et al.*, *Phys. Rev. D* **66**, 033003 (2002); E. Arik *et al.*, hep-ph/0502050.
- [9] D. Acosta *et al.* (CDF Collaboration), *Phys. Rev. D* **71**, 032001 (2005).
- [10] In the CDF coordinate system, θ and ϕ are the polar and azimuthal angles, respectively, with respect to the proton beam direction (z axis). The pseudorapidity η is defined as $-\ln \tan(\theta/2)$. The transverse momentum of a particle is $p_T = p \sin\theta$. The analogous quantity using calorimeter energies, defined as $E_T = E \sin\theta$, is called transverse energy.
- [11] D. Acosta *et al.* (CDF Collaboration), hep-ex/0508029.
- [12] D. Acosta *et al.* (CDF Collaboration), *Phys. Rev. D* **71**, 051104 (2005).
- [13] The missing transverse energy, \cancel{E}_T , is defined as $|\sum E_T^i \hat{n}_i|$, where \hat{n}_i is the unit vector in the transverse plane pointing from the interaction point to the energy deposition in calorimeter cell i .
- [14] The calorimeter isolation I_{cal} is defined as the extra energy deposited in the calorimeter cone of radius $\Delta R = \sqrt{\Delta\phi^2 + \Delta\eta^2} = 0.4$ around the lepton cluster. The I_{cal} is required to be less than 10% of the lepton E_T . The track isolation I_{trk} is defined as the sum p_T of all the tracks in a cone of radius $\Delta R = 0.4$ around the lepton candidate track, but excluding it. The I_{trk} is required to be less than 10% of the lepton track p_T .
- [15] A jet is defined as a cluster of calorimeter towers above an energy threshold of 3 GeV, within fixed radius $\Delta R = 0.4$. The jet E_T is corrected for the calorimeter response and multiple interactions. See A. Bhatti *et al.*, hep-ex/0510047 [Nucl. Instrum. Methods Phys. Res., Sect. A (to be published)].
- [16] T. Sjöstrand *et al.*, *Comput. Phys. Commun.* **135**, 238 (2001). We use PYTHIA V6.2.
- [17] R. Brun and F. Carminati, CERN Program Library Long Writup W5013, 1993 (unpublished).
- [18] We compared the acceptances obtained using MRST 72 and 75 parton distribution functions sets, corresponding to $\alpha_s = 0.1175$ and 0.1125. Also we include the effect of the eigenvector variations around the fit minima, using CTEQ6M PDF sets.
- [19] S. Klimenko, J. Konigsberg, and T. Liss, Fermilab Report No. FERMILAB-FN-0741, 2003; D. Acosta *et al.*, *Nucl. Instrum. Methods Phys. Res., Sect. A* **494**, 57 (2002).
- [20] D. Acosta *et al.* (CDF Collaboration), *Phys. Rev. Lett.* **94**, 211801 (2005).
- [21] J. M. Campbell and R. K. Ellis, *Phys. Rev. D* **60**, 113006 (1999).
- [22] M. Cacciari *et al.*, *J. High Energy Phys.* **04** (2004) 068; N. Kidonakis and R. Vogt, *Phys. Rev. D* **68**, 114014 (2003).
- [23] U. Baur and E. L. Berger, *Phys. Rev. D* **47**, 4889 (1993).